

# Development of a Miniaturized Fiber-optic LDV Sensor for Local Blood Velocity Measurement

## Local Velocity and Flow Profile Measurement of Pulsatile Blood Flow Modeled in Humans

Shimpei Kohri<sup>\*1</sup>, Tsutomu Tajikawa<sup>2</sup>, Kenkichi Ohba<sup>2</sup>

<sup>\*1</sup>Department of Medical Engineering, Aino University 4-5-4, Higashiohda, Ibaraki city, Osaka 567-0012 Japan

<sup>2</sup>Department of Mechanical Engineering, Kansai University, 3-3-35 Yamate-cho, Suita-shi, Osaka 564-8680 Japan

<sup>\*1</sup>s-kohri@me-u.aino.ac.jp

**Abstract-** A novel, less invasive, miniaturized fiber-optic laser Doppler velocimetry (LDV) sensor, which can be directly inserted into a blood vessel was developed for clinical use in measurements of local blood velocity. A convex lens-like surface was formed by a chemical etching on the fiber's tip that had a core diameter of 50  $\mu\text{m}$ . A laser beam that was emitted from the fiber's tip was focused and formed the measuring volume. This fiber sensor was inserted at an insertion angle of 60° through an injection needle, into the flow duct of an acrylic pipe in which highly concentrated fluid, such as whole blood, was flowing in a pulsatile manner. The flow was modeled after human middle cerebral arterial flow. In this study, the local flow velocity and velocity profile across the duct were measured in the pulsatile flow of a dense suspension of a white pigment. The results were compared both with the results obtained using a fringe-mode LDV and with the results that were calculated on the basis of Womersley's oscillatory flow theory. Consequently, it was found that the local velocity and its profile in the pulsatile flow can be successfully measured using the present fiber-optic LDV sensor, which proved the capability of the sensor as a diagnostic device.

**Keywords-** *Fiber-optic LDV Sensor; Pulsatile Flow; Blood Fluid; Local Velocity Measurement*

### I. INTRODUCTION

Measurement of local arterial blood velocity has medical importance as it enables the evaluation of blood flow properties and the detection of blood vessel diseases. There are two measurement methods, the ultrasound Doppler (USD) method and the laser Doppler velocimetry (LDV) method, which do not require calibration for the measurement and the calculation of the flow velocity. The USD method is widely used at clinical sites because using this method, it is possible to measure blood velocity in a non-invasive and safe manner. However, because of its somewhat large spatial resolution of several millimeters, this method is not suitable for the measurements of local velocity. In contrast, the LDV method has a very fine spatial resolution of several micrometers as well as high temporal resolution, making it possible to perform continuous measurements of local instantaneous velocity. Using the conventional fringe-mode LDV, it is possible to measure the velocity by emitting and focusing two laser beams from the duct wall outside the measurement point and by forming the fringe, which the scattering particles cross beyond, to thereby obtain a Doppler signal that is proportional to the velocity. Generally, fringe-mode LDV measurements are performed under the condition of a transparent flow duct wall, and pellucid fluid is used as a working fluid in order to form the fringe at the measurement point in the flow duct. However, laser light is easily absorbed by living tissue such as the skin, bones, muscles and erythrocytes in blood. After the light penetrates about 0.3 mm into blood, its intensity decays dramatically. When fringe-mode LDV is used, laser beams need to pass through the skin and the outer side of the vessel wall, to be focused in the blood; thus, the intensity of the light is remarkably decreased and the measurement of velocity is not possible. Therefore, the fringe-mode LDV cannot be used as a diagnostic device for blood flow velocity measurements. A fiber-optic LDV sensor has been developed as an alternative laser sensor that uses the LDV method [1-4]. Although this sensing method requires the sensor head to be inserted directly into the blood vessel, the associated risk is very low, because the optical fiber, as a sensor head, owing to its small diameter of 125  $\mu\text{m}$ , can be easily and safely inserted into vessels for clinical use by using a catheter or a needle. In addition, these fibers are characterized by good flexibility, light weight, and high resistance to water and corrosion, and are non-inductive and prevent crosstalk. These characteristics are beneficial as they allow the measurement of the blood velocity in a vessel less invasively and more accurately at clinical sites, where different pieces of electronic equipment are at work. However, some serious problems remain because light is easily absorbed in the blood, and multiple scattering events can occur due to the high concentration of erythrocytes in blood (human standard hematocrit  $H_{ct} = 45\%$  which is the percentage of the total volume of blood occupied by blood cells of mainly erythrocytes, leukocytes and platelets). In order to overcome these shortcomings, we have developed herein, a novel and improved fiber-optic LDV sensor, using which we were able to measure the flow velocity of a highly concentrated suspension such as blood [5, 6]. This sensor had a convex lens-like surface on its tip, which allowed the emitted light from the sensor to be focused and to form a very small sampling volume at the point where the intensity of the light was highest. Using the present sensor, we performed in vitro measurements of the local velocity and flow profile of modeled blood flow. The results are discussed using the numerical analysis results and the results that are obtained for the fringe-mode LDV sensor by using the suspension fluid

composed of saline and a few scattering particles, for which the experimental conditions are the same as those used for the fiber-optic LDV sensor .

## II. FABRICATION OF A SENSOR PROBE

A graded index multimode fiber (Sumitomo Electric Industries, Ltd) was used as an LDV sensor probe [7]. Its specifications are shown in Table 1. For blood velocity measurements, a laser beam that is emitted from the sensor's tip needs to be focused at several hundred micrometers in front of the tip because of the high absorption of the light by blood. In this study, the GI fiber tip was fabricated to have a convex lens-like surface by chemical etching using hydrofluoric acid and ammonium fluoride. During the etching process, a GI fiber of flat surface was only soaked in an etchant composed of HF, NH<sub>4</sub>F, and H<sub>2</sub>O, as shown in Fig. 1 (a). The composition rate and etching time were HF: NH<sub>4</sub>F: H<sub>2</sub>O= 0.2:1.0:0.5 and  $t_{\text{etch}} = 5$  hours, respectively. These values were determined using the methods described in previous studies [6, 8]. Fig. 1 (b) shows the microscopic image of a fiber tip used as a sensor, which was fabricated by chemical etching to have convex lens-like surface. The radius of the tip's curvature was 16.9  $\mu\text{m}$ . Fig. 1 (c) shows the optical path of the light that was emitted from the fiber tip in the saline, which had a refractive index of  $n_{\text{saline}} = 1.33$ . The emitted light was focused at 170  $\mu\text{m}$  in front of the fiber. The diameter and the confocal length of the sampling volume (of cylindrical shape) that was formed at the focus point were  $d_s = 2.74 \mu\text{m}$  and  $l_c = 18.4 \mu\text{m}$ , respectively. Using this fiber as a sensor probe made it possible to obtain a Doppler signal with a higher signal to noise ratio in velocity measurements for highly concentrated suspensions including blood, while it was not possible to perform these measurements using the fiber that had a flat tip.

TABLE 1 SPECIFICATION OF A GI-TYPE OPTICAL FIBER

Core material	Ge doped quartz glass
Core diameter	50 $\mu\text{m}$
Cladding material	Quartz glass
Cladding diameter	125 $\mu\text{m}$
Primary coating material	UV curable acrylate
Primary coating diameter	250 $\mu\text{m}$
NA	0.21
Allowable stress	5 kgf
Bending radius	15 mm
Attenuation	1~3 dB/km

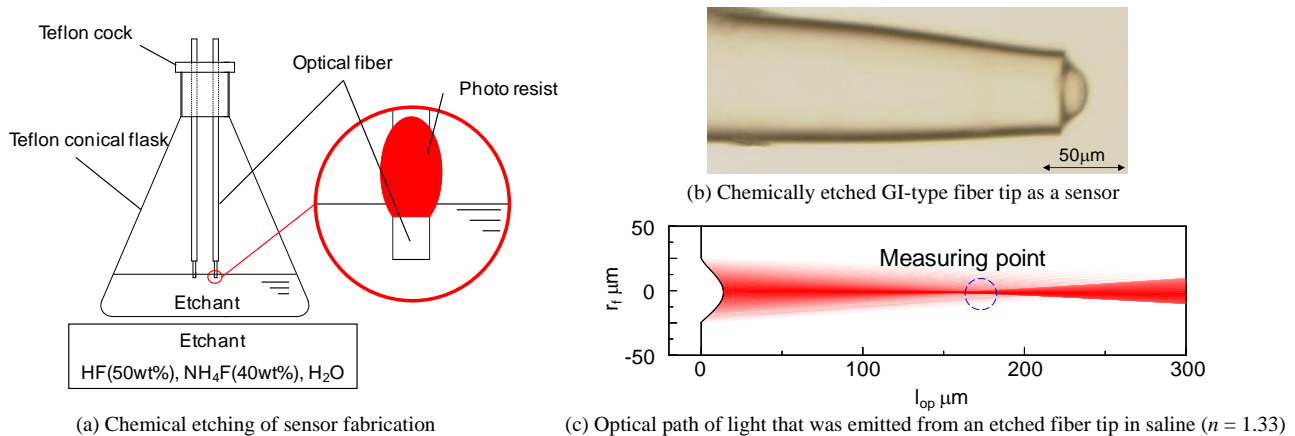


Fig. 1 Fabrication method and specifications of the present fiber-optic LDV sensor

## III. EXPERIMENTAL METHOD

### A. Measurement Principle (Doppler model)

In Fig. 2, a Doppler model of the present fiber-optic LDV sensor is shown. Local flow velocity,  $u$ , can be easily calculated with Eq. (1) by measuring the Doppler shift frequency  $f_D$  [3]:

$$u = \frac{f_D \cdot \lambda_0}{2n |\cos \theta|} \quad (1)$$

In Eq. (1),  $\lambda_0$  is the wavelength of the light,  $n$  is the refractive index of the fluid, and  $\theta$  is the insertion angle. The insertion angle is defined as the angle between the incident laser and flow vectors. From previous studies [6, 8], the insertion angle was determined to be  $\theta=60^\circ$ , for which a Doppler signal with the highest signal to noise ratio was obtained and the error of the insertion angle made a small contribution to the calculation error.

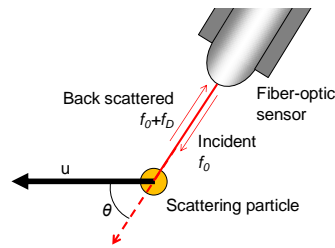


Fig. 2 Schematics of the principle of measurement

### B. Experimental Conditions

Experimental conditions were based on the middle cerebral arterial (MCA) flow [9]. The average velocity of blood flow in the artery was measured using the ultrasound Doppler system (Compumedics Germany GmbH). The measured velocity  $u_{USD}$  is shown in Fig. 3, which was used to set the average flow rate and the pulsatile frequency  $f$  as  $\bar{Q} = 130, 230,$  and  $330$  ml/min and  $f = 1.00, 1.25,$  and  $1.50$  Hz, and the diameter of the model vessel was set as  $3$  mm.

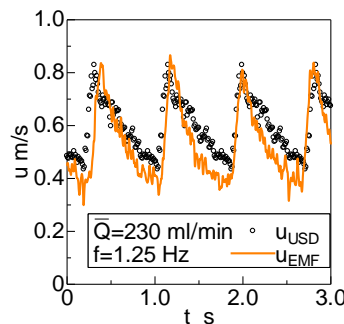


Fig. 3 Cross-sectional velocity waveforms in human middle cerebral artery measured by USD and in experiment by E.M.F.

The properties of blood are not constant but vary among individuals, and it is very difficult to ensure the same physiological and mechanical conditions for different blood flow measurements. In order to perform the experiments under universally acceptable conditions, saline, rather than blood, was used as a working fluid. For an in vitro study of a modeled experiment, it is better to match the Reynolds and Womersley numbers with in vivo values, which can be calculated using the following equations:

$$Re = \frac{u_{ave} \cdot d}{\nu} \quad (2)$$

$$\alpha = \frac{d}{2} \sqrt{\frac{2\pi f}{\nu}} \quad (3)$$

$Re$	: Reynolds number
$\alpha$	: Womersley number
$u$	: average velocity
$d$	: inner diameter of flow duct
$f$	: pulsatile frequency
$\nu$	: kinematic viscosity

In this study, an optical condition of the working fluid's refractive index matching was more important for the evaluation of a fiber-optic LDV sensor, because the focusing length of the sensor depended on the difference between the refractive index of the fluid and the refractive index of the fiber's core. For this reason, and as shown by the data in Table 2, the Reynolds number was four times larger and the Womersley number was two times larger than the corresponding numbers in vivo. Higher Reynolds and Womersley numbers make the flow more disturbed, making it difficult to measure the flow velocity. Therefore, it is plausible to assume that, if local velocity can be measured for the saline using the above sensor, it can be measured in blood as well. Another problem in this experiment emerged because there were no particles that had the same size, form, and scattering properties as erythrocytes in production. White pigments of titanium dioxide (TURNER COLOUR WORKS LTD), of  $2 \mu\text{m}$  in diameter, and of calcium oxide, of  $3 \mu\text{m}$  in diameter, were used as the scattering particles instead of erythrocytes. In the previous study [6], measurements of blood velocity yielded a higher signal to noise ratio as compared to the measurements for the suspension in which the concentration of white pigment was  $20$  g/L. Fig. 4 shows the spectral waveform that is obtained from the spectral analyzer for local velocity measurements that were performed using the fiber-optic LDV sensor. The frequency at the peak denoted by an arrow is the measured Doppler frequency, and the clear peak indicates a high S/N ratio. The broken line denotes the true value of  $f_D$ . Fig. 4 (a) and (b) shows spectral waveforms obtained for the cases of bovine blood of hematocrit  $H_{ct} = 69\%$  and for the suspension in which the concentration of white pigment was  $20$  g/L, respectively. The data shown in this figure were obtained using a fiber tip with a  $21.7 \mu\text{m}$  radius of curvature. In Fig. 4, it is seen that the S/N ratio of a Doppler signal obtained from blood is higher than the S/N ratio obtained from the  $20$  g/L concentrated suspension. These results suggest that by obtaining the signal with a high S/N ratio from the suspension using the sensor, it may be possible to measure the velocity of the blood flow. Fig. 4 (c) shows the spectral waveform obtained using the present

fiber tip, which was an  $r_c = 16.9 \mu\text{m}$  (radius of curvature), and an S/N ratio that is higher than that obtained for  $r_c = 21.7 \mu\text{m}$ .

TABLE 2 COMPARISON OF FLOW PARAMETERS IN BLOOD AND SALINE

		blood	saline
diameter	$d$	3 mm	3 mm
density	$\rho$	1050 kg/m <sup>3</sup>	1000 kg/m <sup>3</sup>
viscosity	$\mu$	4 mPa·s	1 mPa·s
average flow rate	$\bar{Q}$	230 ml/min	230 ml/min
pulsatile frequency	$f$	1.25 Hz	1.25 Hz
Reynolds number	$Re$	428	1630
Womersley number	$\alpha$	2.15	4.20

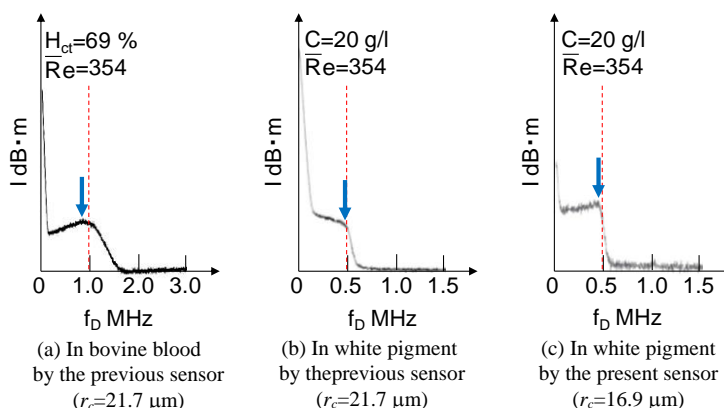


Fig. 4 Comparison of spectral waveforms obtained in velocity measurements

C. Experimental Apparatus

A schematic diagram of the experimental apparatus is shown in Fig. 5. In the flow system, working fluid was pumped by a peristaltic pump (1) to the test section of the acrylic pipe, whose inner diameter was 3 mm. Flow pulsation was generated by the peristaltic pump (2). As shown in Fig. 3, the flow in the experiment was modeled after the middle cerebral arterial flow using the flow valve and the compliance tank, where  $u_{EMF}$  was the average flow rate monitored by an E.M.F. (Electromagnetic Flowmeter, NIHON KOHDEN Corp.). Fig. 6 shows the schematic presentation of the test section. A needle for the insertion of a sensor was incorporated into the acrylic pipe, which was modeled after the MCA flow. The pipe had a small cavity at an angle of  $60^\circ$ . A syringe and an aluminum pipe were fixed on the needle as an insertion guide. Fiber-optic LDV sensor, protected by a stainless steel pipe, was inserted into the flow duct that passed through the guide, and was set at the point of measurement. Using the micro moving device the sensor was moved in the acrylic pipe in steps of 0.05 mm, thus allowing

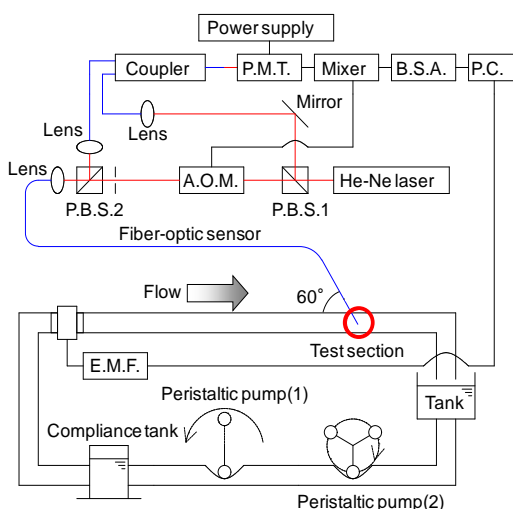


Fig. 5 Schematic diagram of experimental apparatus

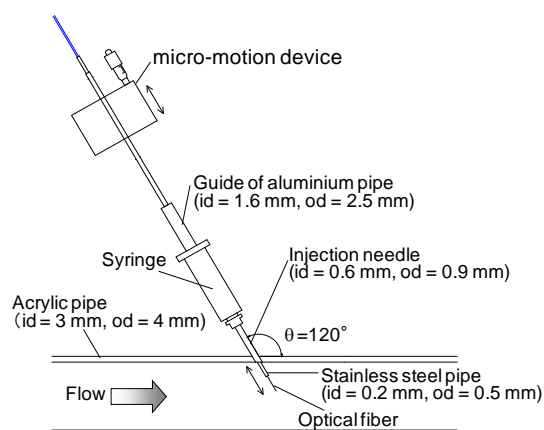


Fig. 6 Schematic diagram of test-section

measurements of flow profile across the duct. The light source was He-Ne laser (NEC Corporation) that had a wave length of  $\lambda_0 = 632.8 \text{ nm}$  and an output power of  $P = 25 \text{ mW}$ . Light emitted from the light source was split by P.B.S. (1) (a polarizing beam splitter) into penetrated light (p-polarized) and reflected light (s-polarized) beams, and intensities of these beams were

controlled by a half-wave plate. The penetrated light was transmitted to an A.O.M. (acousto optic modulator, Intra Action Corp.) and its frequency  $f_0$  was shifted to  $f_0 + 40$  MHz, following which the light ray passed through P.B.S.(2) and entered the fiber sensor. The light was then transmitted through the fiber to the test section and emitted from its convex lens-like surface, which allowed the emitted light to be focused for sampling volume formation. When the scattering particles passed through the sampling volume, the light was scattered and its frequency shifted to  $(f_0 + 40 \text{ MHz}) + f_D$  due to the Doppler effect. The scattered light was detected by the same fiber and was transmitted into the fiber coupler (TATSUTA ELECTRIC WIRE & CABLE CO., LTD.). In contrast, the light beam that was reflected by P.B.S. (1) was transmitted to the fiber coupler as a reference light beam. The scattered light beam and the reference light beam were combined to produce the interference light beam. A P.M.T. (photo multiplier tube, Hamamatsu Photonics K.K.) received the interfered light and converted the intensity of light into the electric signal. The signal was analyzed using the burst spectrum analyzer and was recorded by a personal computer. In order to discuss the accuracy of measurements performed using the present fiber-optic LDV sensor, we performed measurements using the fringe-mode LDV, under the same experimental conditions and with the same flow system, but without the scattering particles. In the fringe-mode LDV measurements, saline was used as a working fluid and a few micro particles with an average diameter of  $10 \mu\text{m}$  (Expancel Inc., DU) were used as scattering particles.

#### D. Womersley's Theory of Oscillating Flow [10]

Pulsatile flow profile in the duct was calculated using Womersley's theory of oscillating flow, and the results of this computation were compared with the results that were obtained using the fiber-optic LDV sensor. Equation (4) shows the expression for the velocity obtained under the calculating conditions of a fully developed laminar flow ( i.e., under these conditions, the radial flow velocity was 0 m/s and the axial flow velocity  $u$  in the axial direction remained constant). In other words,  $u$  is the function of the radial position  $r$  and time  $t$ . In Eq. (4),  $J_0$  is Bessel's function. The coefficients  $A_0, A_1, \dots, A_\infty$  were calculated from Eq. (5):

$$u = \frac{A_0}{4\nu}(a^2 - r^2) + \sum_{n=1}^{\infty} \frac{a^2 A_n}{i\nu\alpha_n^2} \left[ 1 - \frac{J_0\left(i^{\frac{3}{2}}\alpha_n \frac{r}{a}\right)}{J_0\left(i^{\frac{3}{2}}\alpha_n\right)} \right] e^{in\omega t} \quad (4)$$

$$-\frac{1}{\rho} \frac{\partial p}{\partial x} = A_0 + \sum_{n=1}^{\infty} A_n e^{in\omega t} \quad (5)$$

The pressure gradient  $\partial p/\partial x$  was a ratio of the differential pressure and the distance between the points at which the pressure was measured. The difference  $\Delta p$  was obtained by measuring the up-stream and the down-stream pressures at a 0.4 m distance from the test section, and was calculated as  $\Delta p = p_{up} - p_{down}$ . Results of pressure measurements are shown in Fig. 7. The difference  $\Delta x$  was 0.8 m. The tube radius was 1.5 mm, the density of the working fluid was  $1000 \text{ kg/m}^3$ , and the kinematic viscosity  $\nu$  was  $10^{-6} \text{ m}^2/\text{s}$ . The pulsatile flow profile was calculated by using Mathematica5.2 (Wolfram Research Inc.).

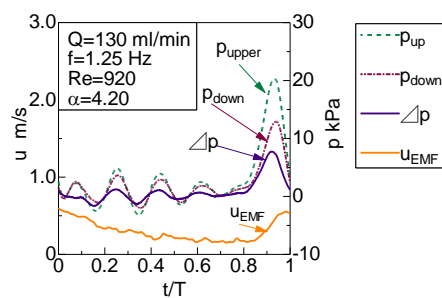


Fig. 7 Pressure waveforms measured for the theoretical analysis

#### IV. RESULTS AND DISCUSSION

Fig. 8 shows the measurement results at the center of the flow duct ( $r = 0 \text{ mm}$ ) under the conditions of pulsatile frequency  $f = 1.25 \text{ Hz}$  and  $\bar{Q} = 130, 230, \text{ and } 330 \text{ ml/min}$ . In Fig. 8,  $u_{FO}$  denotes the local velocity that was measured using the present sensor,  $u_{EMF}$  is the average flow velocity that was calculated from the flow rate, and  $u_{fr}$  is the local velocity that was measured using the fringe-mode LDV. The velocity  $u_{fr}$  was measured separately from  $u_{FO}$ , at the same position, under the same experimental conditions, but without the scattering particles present. These measurements confirm that, for the first time, the

present fiber-optic LDV sensor is able to obtain the Doppler frequency and to measure the local velocity of a pulsatile flow in a highly concentrated suspension. The measured velocity  $u_{FO}$  showed pulsatile dependence on time, and no temporal delay was found between the different velocities by comparing the temporal phase of  $u_{FO}$  with those of  $u_{EMF}$  and  $u_{fr}$ , indicating that the present fiber-optic LDV sensor had a sufficiently high temporal resolution. Under the conditions of  $\bar{Q} = 130$  ml/min, the  $u_{fr}$  and  $u_{W_0}$  were in a good agreement while  $u_{FO}$  attained lower values because the flow was disturbed and separated by the insertion of the sensor. In a fast flow, the flow separation point was moved backward. Thus, higher flow rate or flow velocity resulted in smaller error, as is shown in Fig. 8 for  $\bar{Q} = 230$  ml/min in which there was a good agreement between the values of  $u_{FO}$  and  $u_{fr}$ . For  $\bar{Q} = 330$  ml/min, during the diastole, the period of flow rate decreased, along with a sharp decay in  $u_{FO}$ . These trends were confirmed both for  $u_{FO}$  and for  $u_{fr}$ . This indicated that the descent can be considered to be caused by the characteristic of the flow field. For  $\bar{Q} = 330$  ml/min, the flow in the duct was considered to be temporary turbulent flow. The Reynolds number became  $\sim 3200$  for the maximal flow rate, meaning that the flow in the duct was transitional or turbulent flow. The effect of the flow fields was pronounced when the flow rate was decreasing because those flows did not immediately return to the laminar flow.

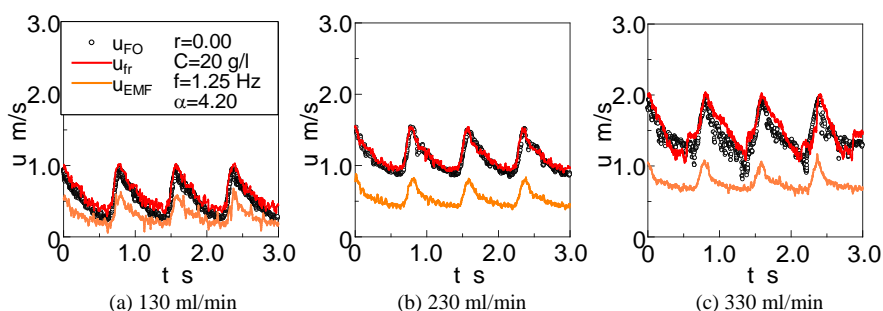


Fig. 8 Waveforms of local flow velocity measured using the present fiber-optic LDV sensor

Flow profiles in the duct are shown in Figs. 9, 10, and 11. In these figures, the ordinate is the local velocity  $u$ , the abscissa is the position  $r$  in the duct, and  $t/T$  is the time that is normalized with respect to the pulsatile period  $T$ . In the measurements that were performed near the wall against the sensor inlet, the sampling volume was positioned in a narrow space surrounded by the wall and sensor head, which caused acceleration of the local flow and made the velocity  $u_{FO}$  higher than  $u_{fr}$ . The velocity  $u_{W_0}$  in Fig. 9 was calculated using Womersley's theory of oscillating flow, which could be employed for laminar flow at any  $t/T$ . For  $\bar{Q} = 130$  ml/min, there was a good agreement between  $u_{FO}$ ,  $u_{fr}$ , and  $u_{W_0}$  during the period  $0 \leq t/T \leq 0.2$ ; however, the value of  $u_{FO}$  was less than values of the others during the period  $0.4 \leq t/T \leq 0.8$  due to the disturbance caused by sensor insertion, with the maximal error becoming 30%. For  $\bar{Q} = 230$  ml/min,  $u_{FO}$  was in a good agreement with  $u_{fr}$ . The experimental condition of  $\bar{Q} = 230$  ml/min and  $f = 1.25$  Hz describes the typical blood flow condition in human MCA; thus, it was concluded that the present fiber-optic LDV sensor could be used as a clinical device for high accuracy measurements of blood velocity. However, for  $\bar{Q} = 230$  ml/min there was a slight difference between the measured velocities  $u_{FO}$  and  $u_{fr}$  and the theoretically calculated velocity  $u_{W_0}$ . This difference could be explained by noting that in the above experimental conditions the flow in the duct temporarily became a transitional, rather than a laminar flow, because in the systolic period near  $t/T = 0$  ( $t/T = 1$ ), the Reynolds number became  $\sim 2400$ . By this reasoning, the experimental radial velocity attained non-zero

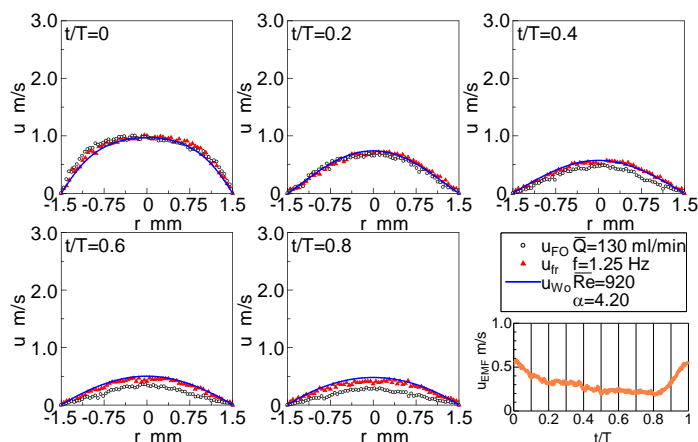


Fig. 9 Velocity profiles of pulsatile flow in  $f=1.25$  Hz and (a)  $\bar{Q} = 130$  ml/min

values, and the computational conditions (for which we assumed zero radial velocity) were not consistent, making the calculated velocity  $u_{w0}$  differ by a small error. For  $\bar{Q} = 330$  ml/min,  $u_{FO}$  and  $u_{fr}$  exhibited some fluctuations, and  $u_{FO}$  was smaller or larger than  $u_{fr}$  at each point of normalized time, with the maximal error reaching 15%. This error was due to the interaction of sensor insertion and temporal transitional or turbulent flow, for which the  $u_{w0}$  was not correctly calculated; as a result, there was a large difference between the measured velocities and the calculated ones. The flow rates  $\bar{Q}_{FO}$  and  $\bar{Q}_{fr}$  plotted in Fig. 12 were calculated by rotational integration of the flow profile and by summing the results obtained at each point of normalized time. For  $\bar{Q} = 130$  ml/min, the error ratio was estimated to be -20% because of the disturbance and separation of the flow by the sensor insertion. For  $\bar{Q} = 230$  ml/min, the acceleration of the velocity near the wall against the sensor inlet made the error somewhat larger. For  $\bar{Q} = 330$  ml/min, the flow disturbance velocity balanced the acceleration of the velocity near the wall; as a result, the error ratio was smaller compared to other conditions. For all experimental conditions, the error ratio of the flow rate was set to  $\pm 20\%$ . Those errors can be reduced by improving the curvature radius of the convex lens, which makes the focal length longer and may allow avoiding the disturbance associated with sensor insertion.

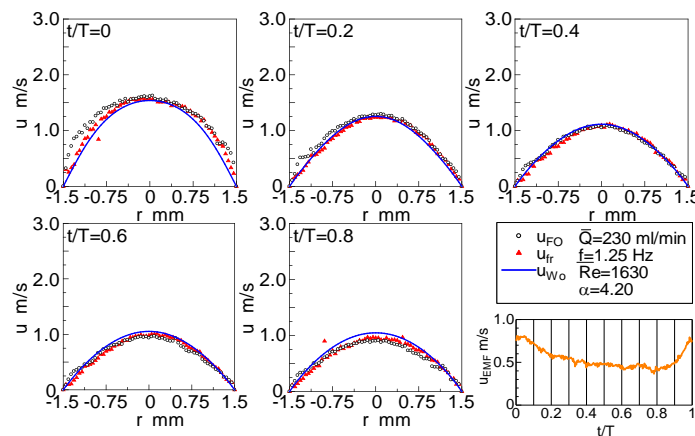


Fig. 10 Velocity profiles of pulsatile flow in  $f=1.25$  Hz and  $\bar{Q} = 230$  ml/min

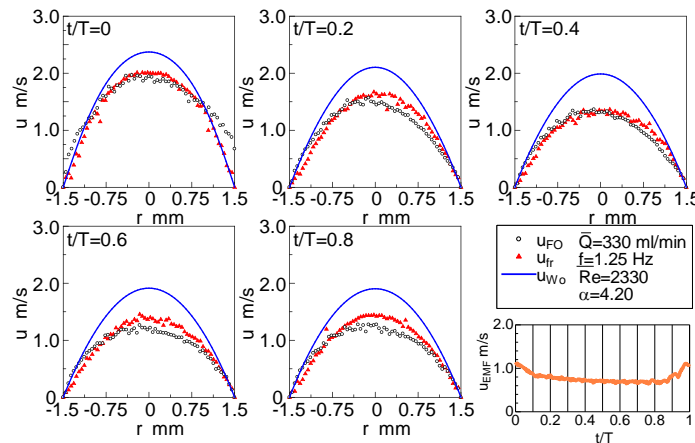


Fig. 11 Velocity profiles of pulsatile flow in  $f=1.25$  Hz and (a)  $\bar{Q} = 330$  ml/min

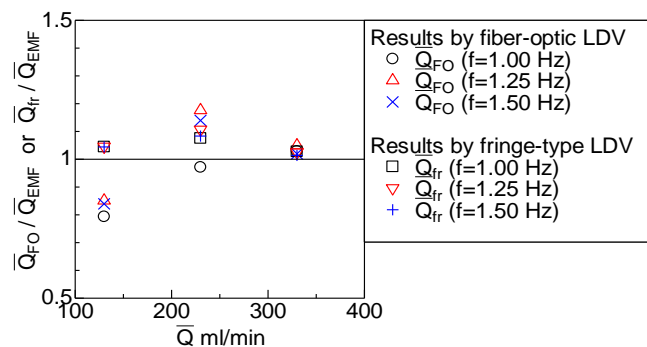


Fig. 12 Error ratio of the flow rate calculated from the flow profile

## V. CONCLUSIONS

A novel, less invasive, miniaturized fiber-optic LDV sensor was developed for measurements of human pulsatile flow velocity. The sensor had a convex lens-like surface on a fiber tip that was 50  $\mu\text{m}$  in diameter. Using the present sensor, a Doppler shift frequency corresponding to the local velocity was accurately obtained in the working fluid of a highly concentrated suspension, which represented the same degree of optical difficulty for laser-based measurements as blood erythrocytes. Local velocity and flow profile were successfully measured in the pulsatile flow modeled after human middle cerebral arterial flow, indicating that the present sensor could be used to measure the local velocity of whole blood flowing in the human body. Considering the important advantages of sensor minuteness, its ability to perform measurements in blood, and its very high spatial and temporal resolutions, the present fiber-optic LDV sensor for local blood measurement promises to become an intrinsic component of the medical equipment used at clinical sites. In addition, by utilizing the optical fiber's characteristic resistance to water, heat, corrosion, and electricity, the developed sensor is likely to become useful in several ways, such as in industrial, and chemical applications.

## REFERENCES

- [1] T. Tanaka, and GB. Benedek, "Measurement of the Velocity of Blood Flow (in Vivo) Using a Fiber Optic Catheter and Optical Mixing Spectroscopy", *Applied Optics*, vol. 14, pp. 189-196, 1975.
- [2] K. Nishihara, J. Koyama, N. Hoki, F. Kajiya, M. Hironaga, and M. Kano, "Optical-Fiber Laser Doppler Velocimeter for High-Resolution Measurement of Pulsatile Blood Flows", *Applied Optics*, vol. 21, iss. 10, pp. 1785-1790, 1982.
- [3] K. Ohba, and N. Fujiwara, "Development of Fiber Optic Laser Doppler Velocimeter for Measurement of Local Blood Velocity", *SPIE Laser Anemometry Advances and Applications*, vol. 2052, pp. 195-201, 1993.
- [4] H. Cai, A E. Larsson, and P Å. Öberg, "Single Fiber Laser-Doppler Flowmetry—Dependence on Wavelength and Tip Optics", *Journal of Biomedical Optics*, vol. 3, pp. 334-339, 1998.
- [5] L. Scalise, W. Steenbergen, and F de Mul, "Self-Mixing Feedback in a Laser Diode for Intra-Arterial Optical Blood Velocimetry", *Applied Optics*, vol. 40, pp. 4608-4615, 2001.
- [6] T. Tajikawa, W. Ishihara, S. Kohri, and K. Ohba, "Development of Miniaturized Fiber-Optic Laser Doppler Velocimetry Sensor for Measuring Local Blood Velocity: Measurement of Whole Blood Velocity in Model Blood Vessel Using a Fiber-Optic Sensor with a Convex Lens-Like Tip", *Journal of Sensors*, 2012.
- [7] D. Gloge, and E. Marcatili, "Multimode Theory of Graded-Core Fibers", *B.S.T.J.*, vol. 52, iss. 9, pp. 1563-1578, 1973.
- [8] T. Tajikawa, M. Takeshige, W. Ishihara, S. Kohri, and K. Ohba, "Development of Miniaturized Fiber-Optic Laser Doppler Velocimetry Sensor for Measurement of Local Blood Velocity (Fabrication Method for Convex or Concave Lens-Like Fiber Tip and the Characteristics of Sensor Optical System)", *Journal of Fluid Science and Technology*, vol. 4, iss. 1, pp. 62-74, 2009.1.
- [9] Y. C. Fung, *Biomechanics*, Springer-Verlag, New York Heidelberg Berlin, pp. 62-68, 1981.
- [10] J. R Womersley, *Ann. Phil. Mag.* vol. 46, p. 199, 1955.